공학석사학위논문

Bioresorbable Electronic Patch (BEP) Enabled Active Control of Drug Delivery for Brain Tumor Therapy

뇌종양 치료를 위한 능동적인 약물 전달 조절이 가능한 생분해성 전자 패치

2016년 8월

서울대학교 대학원

화학생물공학부

에너지환경화학융합기술전공

서현선

Abstract

Bioresorbable Electronic Patch (BEP) Enabled Active Control of Drug Delivery for Brain Tumor Therapy

Hyunsun Seo

School of Chemical and Biological Engineering

The Graduate School

Seoul National University

Brain tumor disease is one of the harshest human cancers to treat. The presence of blood-brain barrier which prevents penetration of drugs into brain and residual tumors after surgical resection make brain tumor disease still remain unsolvable. Recently, clinical efforts to overcome those limitation of existing treatment of brain tumor disease have reported. Especially, implantable drug delivery system using biodegradable polymer wafer has been clinically used. However, it has serious demerits that the drug delivery is uncontrollable and inefficient. Emerging of

new drug delivery system with active controllability is highly demanding. Here, I demonstrate a bioresorbable electronic patch (BEP) enabled sustainable, controllable, and localized drug delivery for brain tumor therapy. A natural bioresorbable polymer, starch, is fabricated as a form of flexible patch for conformal contact with biological tissues. An anti-cancer drug named doxorubicin (DOX) is loaded in the starch patch. Functional group modification of starch enables sustainable release of drug by forming covalent bonding between starch and DOX. Bioresorbable magnesium (Mg) heater performs wireless RF heating resulting in thermal actuation of drug delivery by breaking the bonding. To prevent excessive heating, real-time temperature monitoring by wireless temperature sensor as a form of LC oscillator is achieved. Therapeutic effects of BEP is verified by *in vivo* demonstration include tumor recurrence analysis using MRI and survival study. Therefore, BEP enabled active control of drug delivery has a great potential for becoming a novel and efficient treatment of brain tumor disease.

Keywords: Bioresorbable patch, Bioresorbable electronics, Brain tumor therapy, Implantable drug delivery system.

Student number: 2014-22593

Contents

List of Schemes

List of Figures

List of Tables

1. Introduction

Glioblastoma multiforme, the most common and malignant tumor disease of brain, is one of the most difficult human cancers to treat. Despite mobilization of all aggressive treatment including surgical resection, radio therapy, and chemotherapy, the median survival after diagnosis is just 12 months and only about 5% of total patients survive after 5 years[1,2]. Because brain plays a pivotal role in life activities, surgeons cannot resect sufficient amounts of brain tissues for complete removal of tumor. Such limitation results in existence of residual tumors after surgery, and thereby tumor recurrence, mostly in the vicinity of primary tumor sites, frequently occurs. Though fluorescence-guided surgery by 5-aminolevulinic acid may increase the accuracy of tumor resection[3], microscopic tumor cells emitting weak fluorescent light to be recognized still remain. Once local recurrence appears, there exists no more appropriate treatment because radiotherapy on same region is forbidden for at least two years and tumor cells already had tolerances to previous chemotherapy drugs. Moreover, drugs cannot be delivered into brain by conventional drug delivery method such as oral ingestion and intravenous injection due to the presence of the blood-brain barrier (BBB)[4].

Recently, some clinical studies for overcoming such limitation of standard treatment of brain tumor diseases have reported. Hyperthermia therapy, a medical

treatment of giving thermal damage to cancer cells, by using magnetic nanoparticles[5,6] has shown some therapeutic effects. However, required temperature to injure cancer cells is so high that adjacent normal brain tissues also be harmed by heating. Magnetic nanomaterials conjugated with anti-cancer drugs also function as drug delivery system[7], but the amount of loading drugs are not enough for expecting therapeutic results. Also, the BCNU polymer (1,3-bis[2-chloroethyl]-1-nitrosourea) wafer approved by Food and Drug Administration (FDA) in 1996 has been clinically used[8]. BCNU polymer wafer consists of an anti-cancer drug named Carmustine and a biodegradable polymer named Polifeprosan20 (PCPP-SA) as a drug reservoir. The wafers are implanted in the cavity of brain to treat residual tumors after resection surgery. Although the wafer has shown some beneficial clinical effects, it still has some serious demerits. Firstly, lifetime is too short. All drugs are released within five days after implantation because the drugs are just physically trapped in polymer matrix and released through pores when polymer starts to degrade. Secondly, the wafer cannot deliver drugs perfectly to the local tumor cells. Due to its rigid and hydrophobic properties, the wafer cannot completely adhere to tumor tissue. Then, drugs are not wholly delivered to the tumor sites, but partially to normal cells. Not only decreased therapeutic effects but also increased side effects may be resulted in. Therefore, development of drug delivery system with active controllability is still demanding to improve the treatment effects and minimize side effects.

In this paper, I demonstrate a bioresorbable electronic patch (BEP) for sustainable, controllable, and localized drug delivery of brain tumor therapy. Getting

ideas from the point that the rice paste is sticky, starch, a natural bioresorbable polymer, is used as a drug reservoir and a matrix of the patch for good adhesion to biological tissues. Starch patch can be fabricated as a flexible form for conformal contact with soft and curvilinear brain tissues. Doxorubicin (DOX), an anti-cancer drug, is loaded in the starch patch both as a physically trapped and a chemically bonded form. Through functional group modification of starch patch in which some hydroxyl groups change into aldehyde groups, DOX can be covalently bonded to starch polymer. Drug release rate can be regulated by adjusting the ratio between the amount of physically trapped and chemically bonded DOX; physically trapped DOX quickly escaped from the patch, on the other hand, chemically bonded DOX are slowly released as covalent imine bonds are broken. Also, modified aldehyde functional group contributes to improve the adhesion onto biological tissues and provide pH sensitivity of drug release for tumor targeting. To actuate the drug delivery as necessary, wireless electronic heater is laminated on the starch patch. The heater made of bioresorbable metal, magnesium (Mg), transforms input radio frequency (RF) energy into thermal energy for elevating temperature of patch so that the covalent bonding between DOX and starch can be broken. In addition, wireless temperature sensor consisting of Mg and biodegradable polymer, poly[lactic-co-glycolic acid] (PLGA), functions as a real-time monitoring of temperature for preventing excessive heating since too much increase of temperature may harm normal cells. Poly lactic acid (PLA) which also has a biodegradability is used as an encapsulation layer to protect electronic components from too fast dissolution and

prevent unnecessary DOX release to the opposite side. A final form of BEP integrated all components mentioned above (Figure 1) is proven its therapeutic effects by *in vivo* animal studies. Human glioblastoma cells are implanted and grown into subcutaneous tissues of mice. Then, for simulating actual usage as a treatment method, BEP is adhere to residual tumors after the majority of tumor tissues are surgically resected. Both tumor recurrence analysis through MRI and survival study show substantial therapeutic effects of BEP. Therefore, BEP enabled active control of drug delivery with complete bioresorbability have a great potential for becoming an innovative and practical treatment of brain tumor disease.

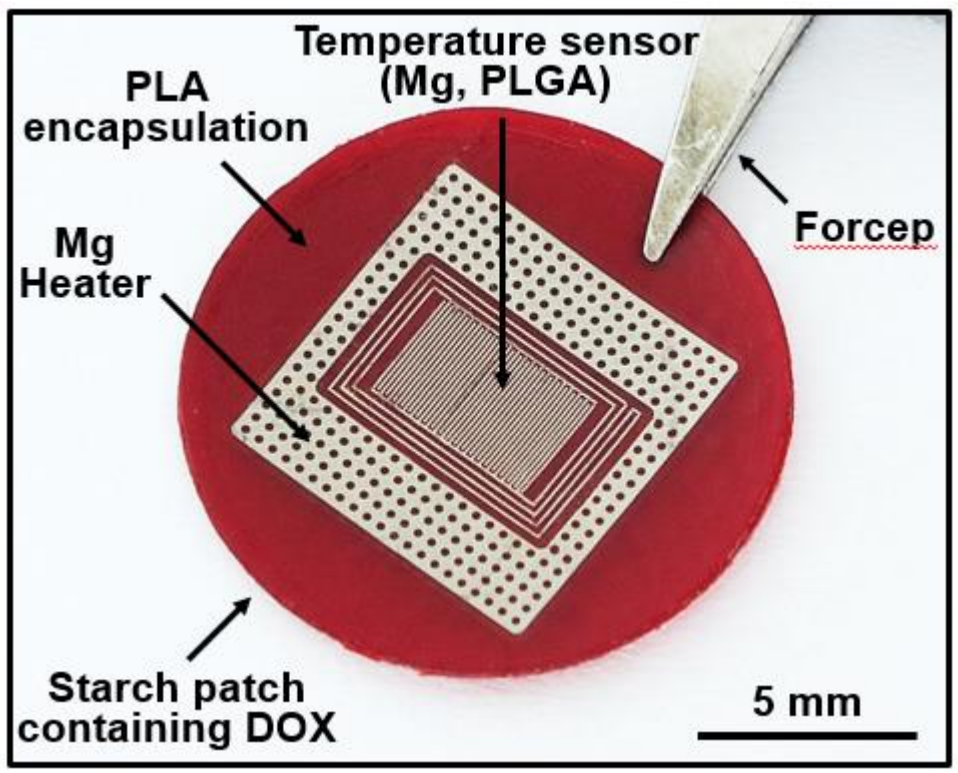

Figure 1. A picture of bioresorbable electronic patch (BEP).

2. Bioresorbable starch patch

2.1. Fabrication of starch patch

Starch polymer is used as a matrix of patch which functions both as an anti-cancer drug, doxorubicin (DOX), reservoir and a substrate of electronic components. Fabrication process of starch patch containing DOX is shown in Figure 2. Proper amounts of starch powder, doxorubicin, glycerol as a plasticizer, and DI water were mixed. Then, mixed solution was dried under appropriate conditions of temperature and humidity (65 ℃ and 80 percentage of humidity) for about 24 hours. Satisfying an optimum ratio between each other is important for forming a patch with desirable mechanical properties. Firstly, lack of water induces starch polymer to absorb all water molecules leading to starch gelatinization[9]. Also, a ratio between glycerol and starch determines the mechanical properties of patch especially related to flexibility. Figure 3 shows elastic modulus and maximum elongation at fracture point of starch patch depending on starch-to-glycerol ratio as a unit of weight percentage. The patch comprising 40% of starch-to-glycerol ratio is chosen for this study.

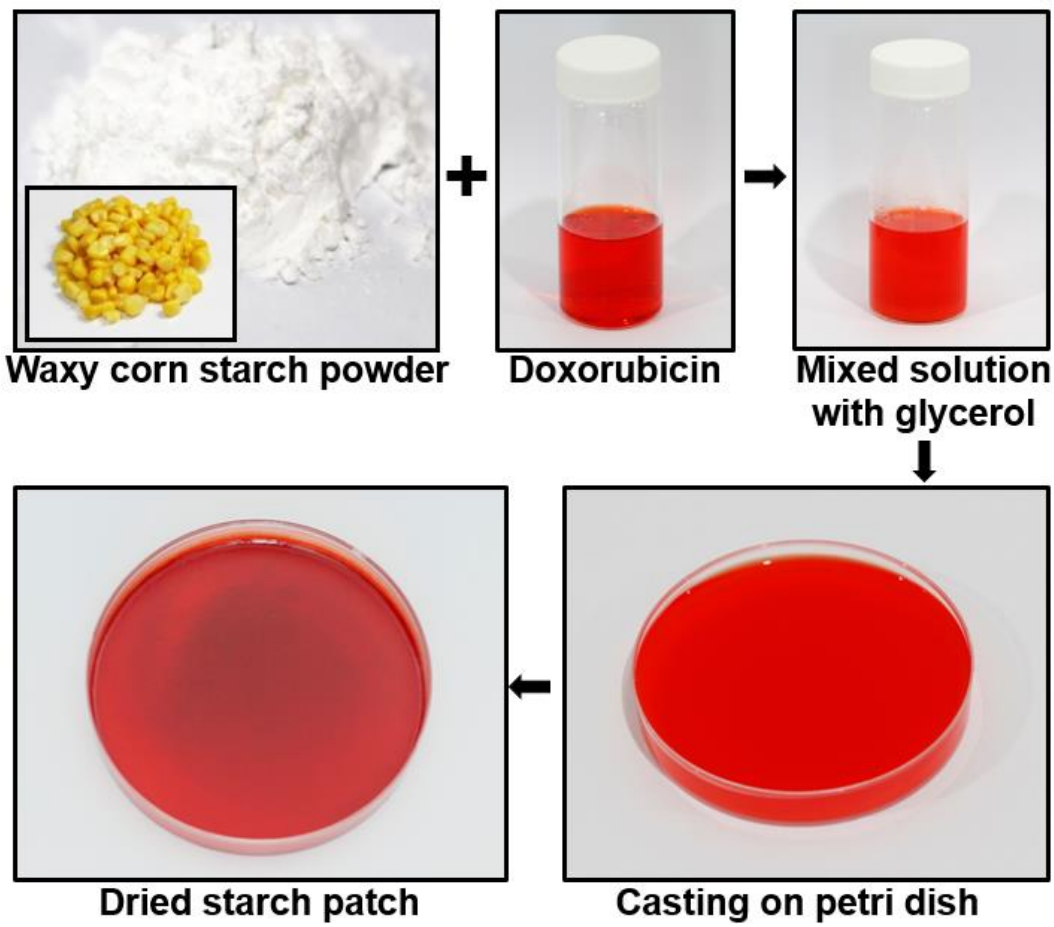

Figure 2. Fabrication of bioresorbable starch patch containing DOX.

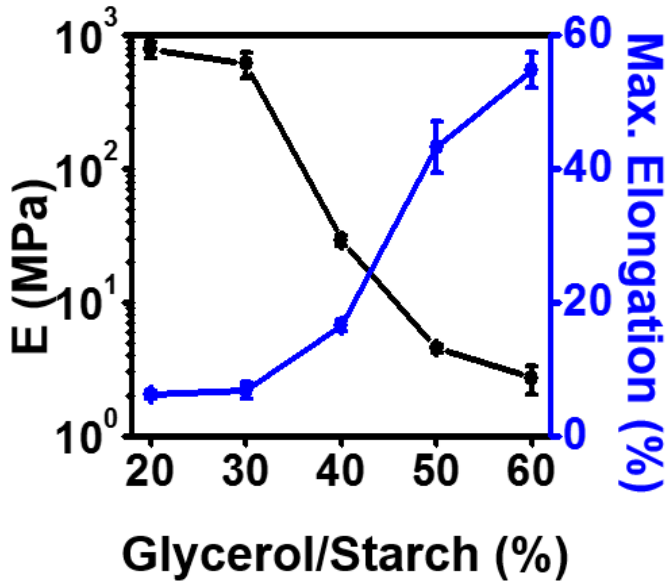

Figure 3. Elastic modulus (black) and maximum elongation (blue) of bioresorbable starch patch.

2.2. Conformal adhesion of starch patch

Conformal contact with biological tissues is positively necessary for efficient and localized drug delivery system (Scheme 1). Fabricated starch patches can be distinguished in magnetic resonance imaging (MRI) if MRI contrast agent is added during fabrication process. Sticky starch patches can be attached to diverse biological organs of rat (Figure 4 right). MRI images clearly display the conformal adhesion of starch patches on soft and curvilinear bio-structures (Figure 4 left). A scanning electron microscope (SEM) image of an interface between cow brain and starch patch (*ex vivo*) presents that the patch completely adheres to brain tissue also in a microscopic view (Figure 5). Furthermore, localized and focused drug delivery due to good adhesion of starch patches was confirmed *in vivo*. A starch patch containing DOX was implanted on the surface of rat brain. After implantation of 24 hours, the brain was extracted and fluorescence signals were observed by IVIS Lumina II (PerkinElmer). DOX fluorescence signals were solely detected in the patch implant site (Figure 6). In other words, this indicates that the delivery of DOX is localized and focused on the area just below the implantation site.

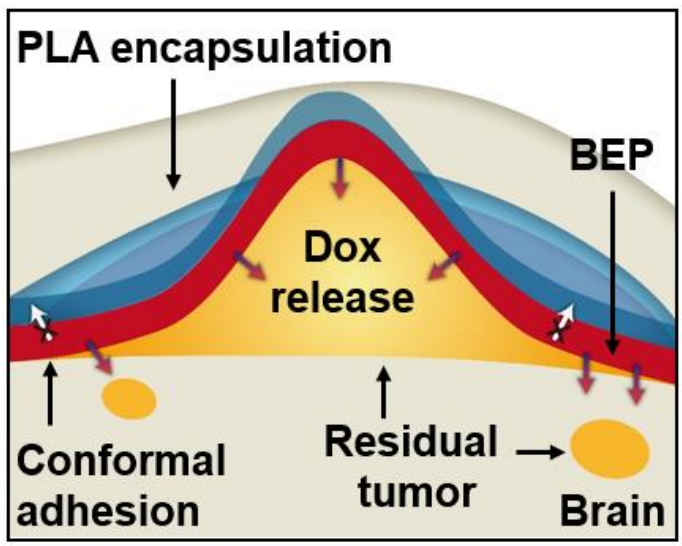

Scheme 1. Conformal adhesion of BEP into brain tissue.

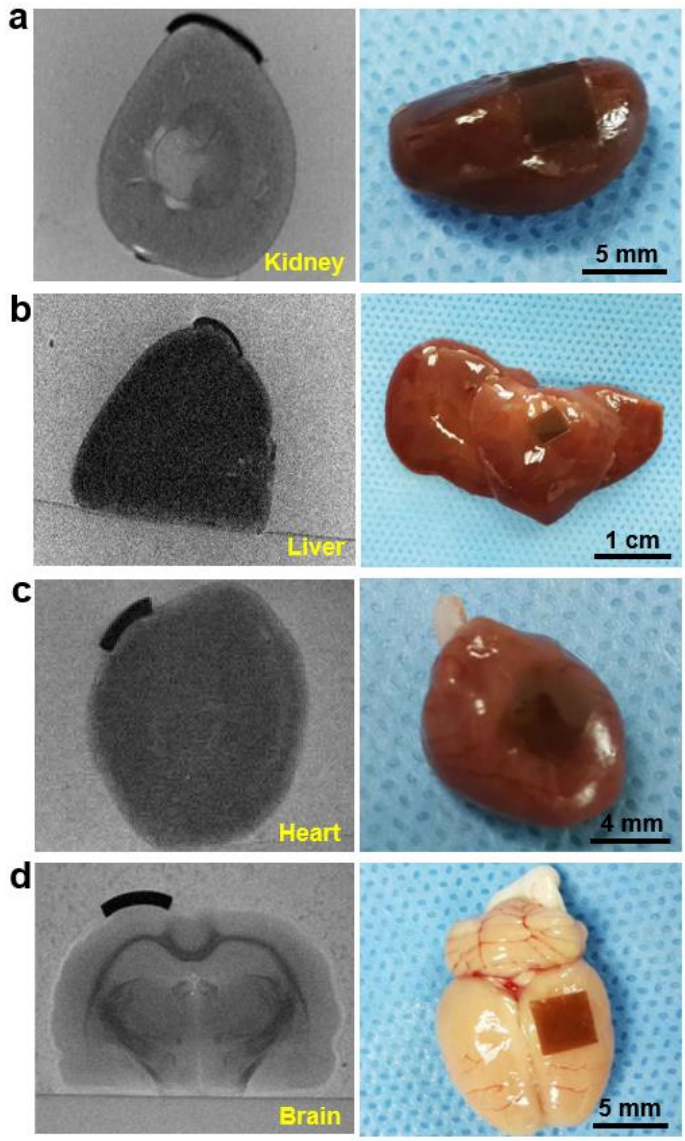

Figure 4. MRI images (left) and pictures (right) of sticky bioresorbable starch patch attached to (a) kidney, (b) liver, (c) heart, and (d) brain of rat.

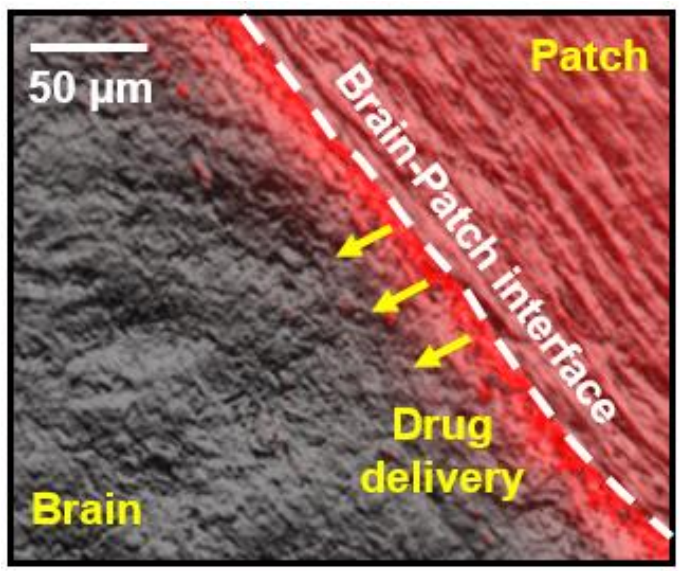

Figure 5. A SEM image of cow brain-starch patch interface.

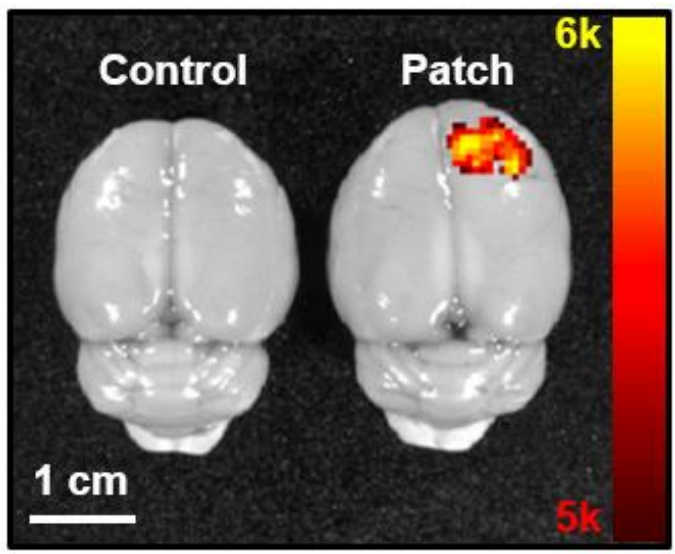

Figure 6. *In vivo* fluorescence image of starch patch containing DOX implanted in rat brain.

2.3. Aldehyde functional group modification of starch

Doxorubicin can be sufficiently loaded in the starch patch, however, they escaped from the patch with the very fast rate when implanted since they are just physically trapped in the starch polymer chain. Accordingly, making a strong interaction between DOX and starch is required to prolong lifetime of the patch for a clinical usage. Through functional group modification of starch, covalent bonding can be formed between DOX and starch. By changing hydroxyl functional groups (-OH) of nature starch polymer into aldehyde groups (-CHO) (Scheme 2a)[10], amine group ($-NH_2$) of DOX can be reacted with the aldehyde group of starch resulting in the formation of imine bonding (C=N) (Scheme 2b)[11,12]. Detailed synthesis method is described in Experimental Section (5.2).

This imine bonding contributes to not only a delayed release of DOX but also increasing adhesive forces to brain tissues and tumor targeted drug delivery. Scheme 3 describes the effects of aldehyde functional group modification of starch. Firstly, as mentioned above, aldehyde groups enable DOX can be chemically bonded to starch chain so that natural release from the reservoir is impeded (Scheme 3iii). Secondly, the aldehyde groups which are not reacted with DOX can also form covalent bonding with amine groups of brain tissues (Scheme 3i). This leads to better adhesion of patch onto brain tissues. Lastly, the imine bonding of starch-DOX gives pH sensitivity of DOX release because hydrogen ions accelerate the decomposition of the bonding (Scheme 3ii[13,14]). Since the microscopic environment in tumor tissue

(pH ~ 6.5-7.2) is more acidic than that in normal tissue (pH ~ 7.4), pH triggered release of DOX near tumor tissues may be possible[15,16].

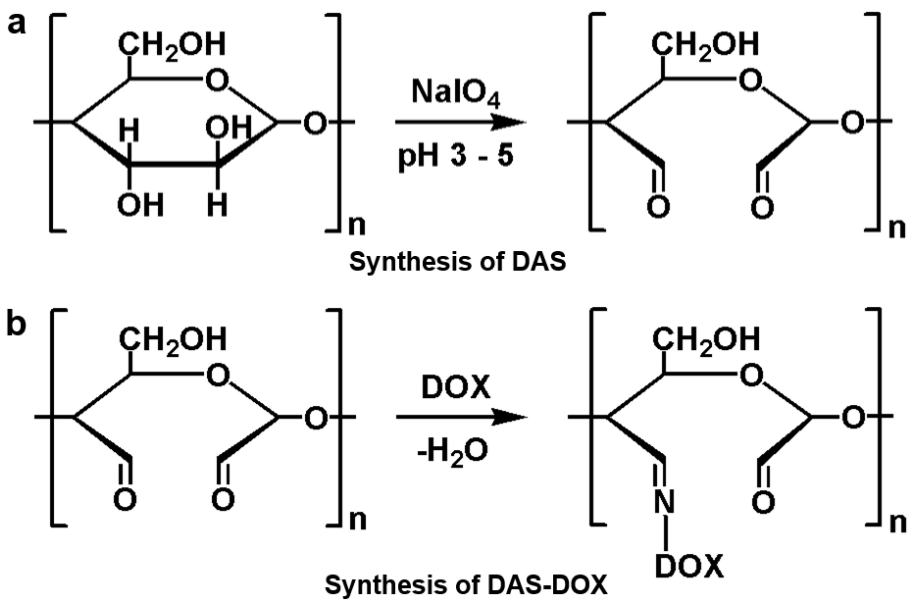

Scheme 2. Synthesis of (a) dialdehyde starch (DAS) and (b) DAS-DOX

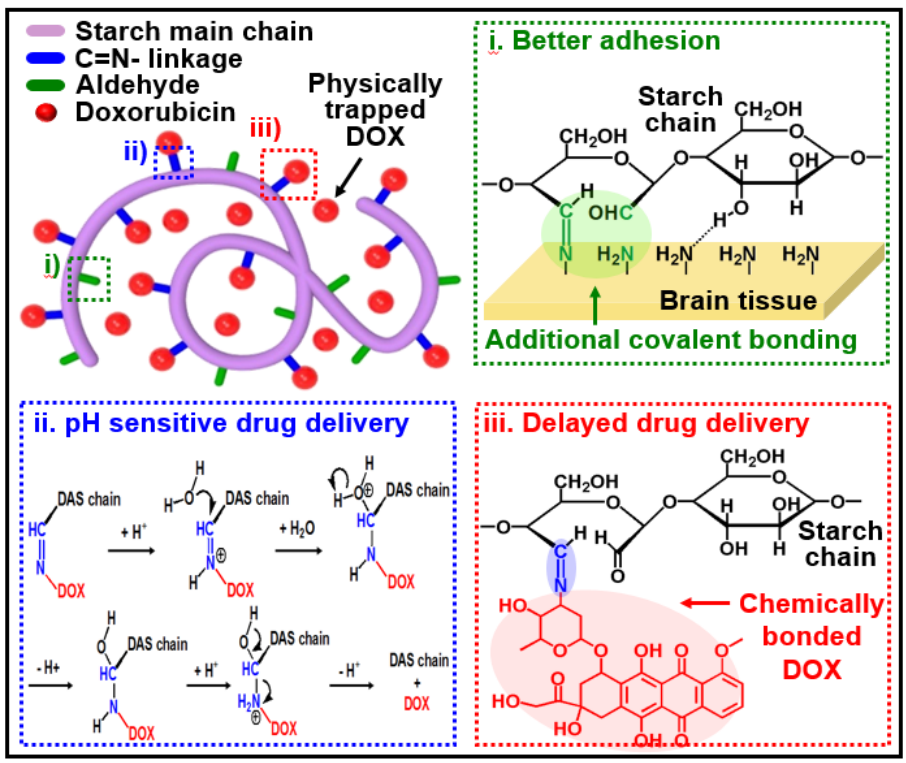

Scheme 3. Effect of aldehyde functional group modification of starch.

2.4. Adhesion test of modified starch patch

Contents of aldehyde functional groups among total hydroxyl groups can be controlled during the synthesis process. To verifying the relation between adhesion force and aldehyde functional groups as mentioned above in Scheme 3i, adhesion test of modified starch patch with different contents of aldehyde group was performed. Each patch was attached to cow muscle and shear stress was measured by a tensile testing machine. The results show that the higher the portion of aldehyde groups increases, the larger the shear stress of the patch becomes (Figure 7). In other words, adhesion force onto cow muscle becomes stronger as aldehyde content is raised. The patch composed of modified starch with 10 % aldehyde groups (~78 kPa) has approximately ten times larger shear stress than that of natural starch (~7 kPa). On the other hand, mechanical properties such as flexibility and fracture toughness become worse as aldehyde content increases more than 10 %. Thus, modified starch with 10 % aldehyde group is chosen for following study. 10 % aldehyde group is also enough for making bonds with sufficient amounts of DOX.

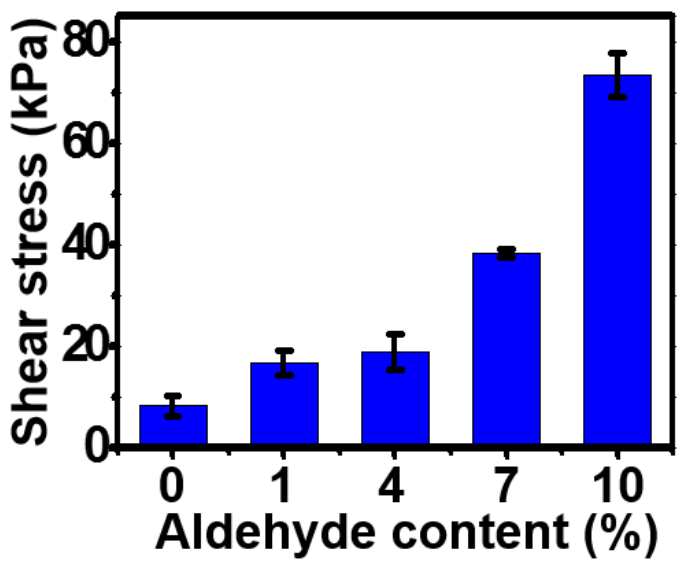

Figure 7. Adhesion test of bioresorbable starch patch.

2.5. *In vitro* drug release profile of modified starch patch

Figure 8 presents DOX release in phosphate-buffered saline (PBS) solution (0.01 M) of natural starch patch (St, black), modified starch patch (DAS, blue), and modified starch patch with full encapsulation by poly lactic acid (PLA) (Encap., red). As mentioned above in 2.3, most of the loaded DOX (~ 90 %) are released within 1 day in case of natural starch patch due to its weak interaction with DOX. On the other hand, initial release of DOX within first day is less than 25 % in case of the patch composed of modified starch with 10 % aldehyde group. This is because only small portion of total DOX amounts is physically trapped while majority of DOX is strongly bound with covalent bonding. Chemically bonded DOX is slowly and continuously released after first day as shown in blue line of Figure 8. To evaluate the effect of PLA encapsulation layer, a modified starch patch is fully encapsulated via dipping into PLA solution. Almost all drugs (more than 95 %) are remaining as shown in red line of Figure 8.

To identify the pH dependence of DOX release from modified starch patch, PBS solution having different pH were prepared. Tendency of the increase in drug release rate according to the decrease in pH was observed (Figure 9). The pH triggered drug release of patch may positively affect the tumor targeted drug delivery. Temperature dependence was also clarified. DOX release in 47 ℃ is more than 2 times faster than that in 37 ℃ which is body temperature (Figure 10). The result implies that covalent bonding between DOX and modified starch may be broken by

applying proper thermal energy. In other words, thermal actuation of DOX release from the patch is possible.

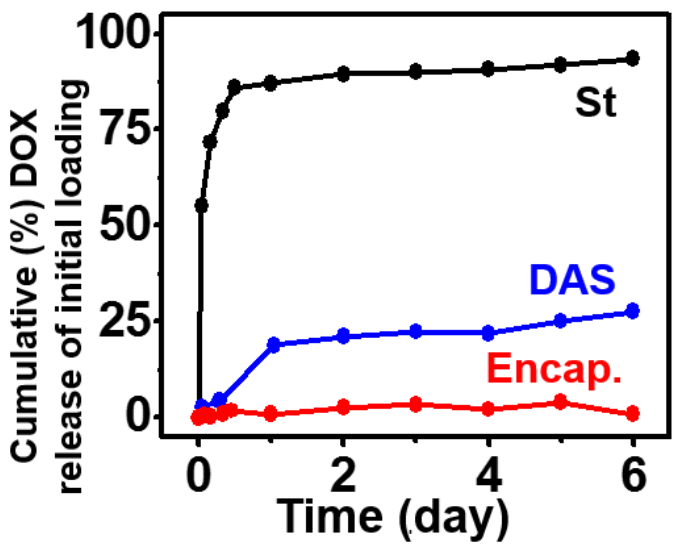

Figure 8. Comparison of *in vitro* drug release profile according to the type of patches. St (black) indicates a natural starch patch. DAS (blue) indicates a patch composed of modified starch with 10 % aldehyde group. Encap. (red) indicates the modified starch patch with full encapsulation by PLA.

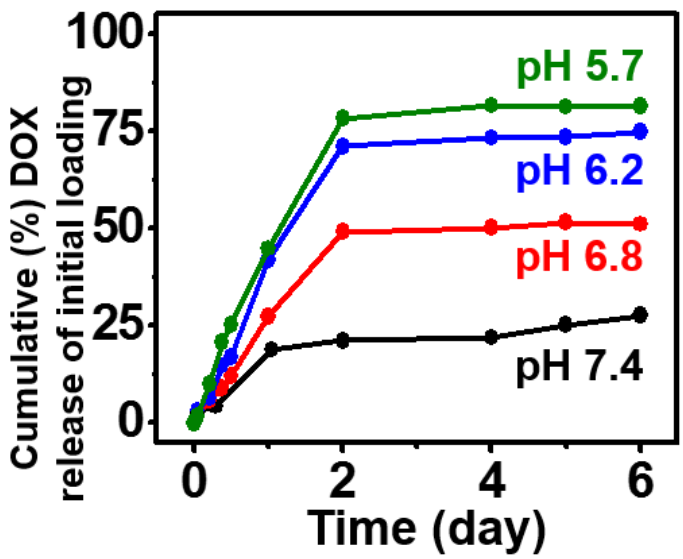

Figure 9. The pH dependence of *in vitro* drug release profile of the modified starch patch.

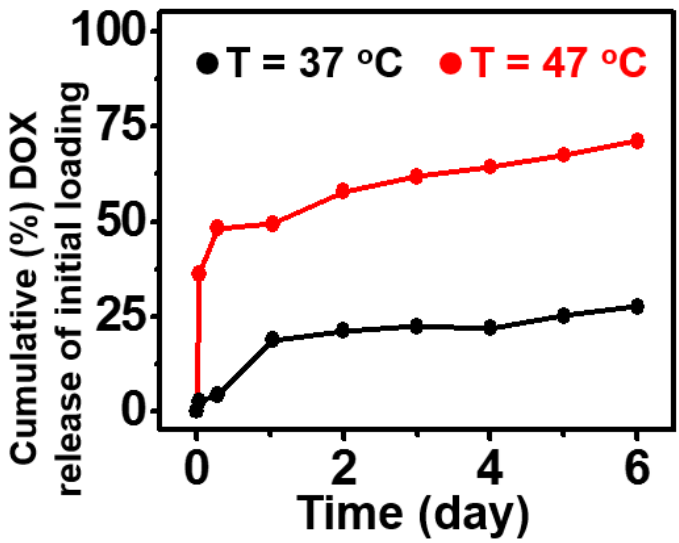

Figure 10. Temperature dependence of *in vitro* drug release profile of the modified starch patch.

3. Bioresorbable wireless electronics

3.1. Wireless RF heating of bioresorbable heater

A wireless heater comprised of bioresorbable metal, Mg functions as an actuator of drug delivery by providing thermal energy to the BEP. Fabricated Mg heater is laminated on the top surface of the starch patch. Detailed information of fabrication of Mg heater is explained in Experimental Section (5.7). PLA encapsulation layer is then covered over the heater for preventing the dissolution before the lifetime has ended. Scheme 4 explains the operation principle of Mg heater on BEP. Magnetic field generated by wireless radio frequency (RF) energy from a RF coil induces eddy current in Mg heater. Then, the heater transforms electrical energy generated by eddy current into thermal energy. The design of heater is optimized for uniform emission of heat.

Figure 11a is an actual picture of wireless RF heating of BEP implanted in the rat brain. An infrared (IR) camera image shows that the heater wirelessly operates very well (Figure 11b). The performance of the heaters with different sizes is evaluated (Figure 12). Obviously, the bigger the size of the heater is, the higher the elevating temperature reaches. The heater with a side length of 6 mm (black) is selected for following animal study since immoderate increasing of temperature damages normal tissues. To determine the appropriate coil distance for the safety of

neighboring tissues, histological analyses stained with an apoptosis inhibitor, survivin, are performed (Figure 13). Almost all cells express survivin when the coil distance is 2 cm (Figure 13a) while there is no cell expressing survivin which means that all cells undergo apoptosis when the coil distance is 0.5 cm (Figure 13c). In case of coil distance of 1 cm (Figure 13b), cells located far from the BEP implanted site are survived but cells adjacent to the BEP undergo apoptosis. Therefore, 2 cm is chosen as the coil distance from the BEP for following animal study,

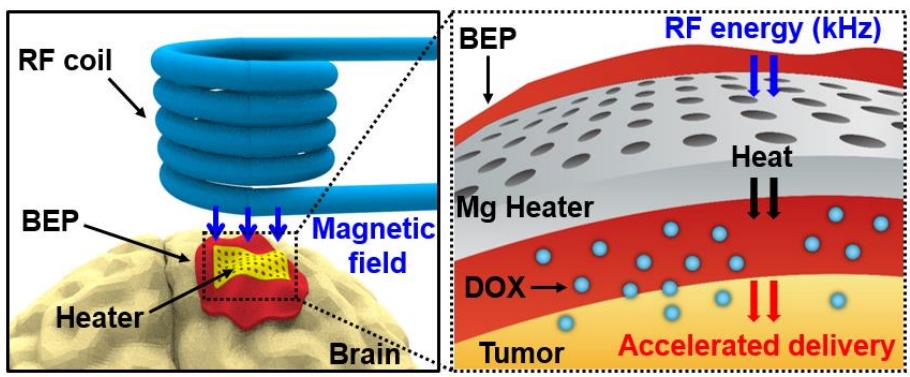

Scheme 4. Wireless thermal actuation of drug delivery using bioresorbable Mg heater.

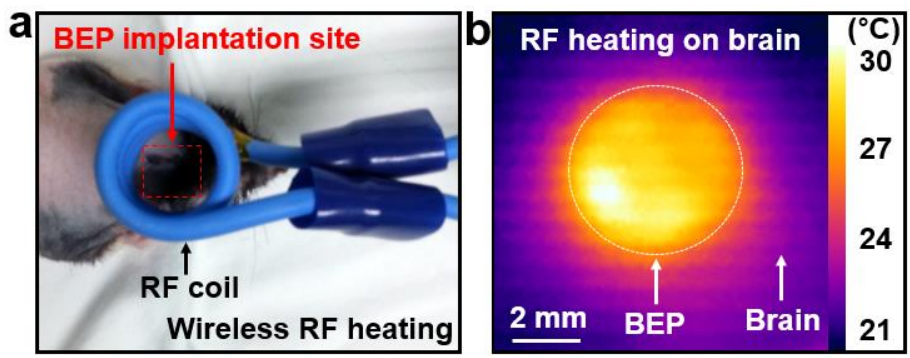

Figure 11. (a) A picture and (b) an infrared (IR) camera image of wireless RF heating of BEP implanted in rat brain.

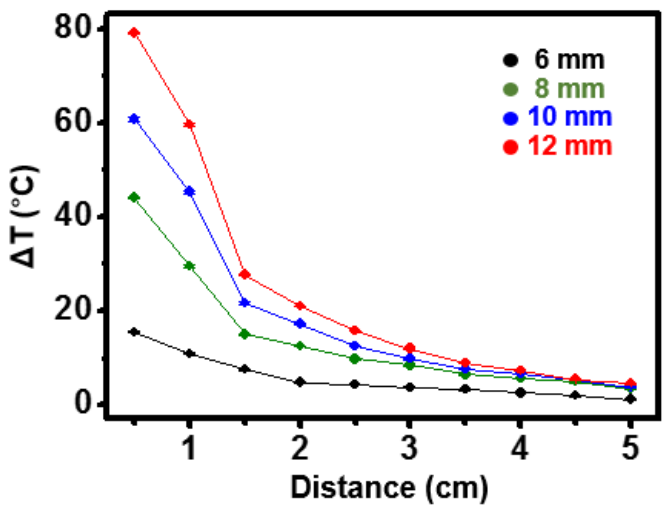

Figure 12. Heating performance of BEP with different sizes of the Mg heaters versus distance between BEP and RF coil. Each number (mm) indicates the length of a side of a square-shape Mg heater.

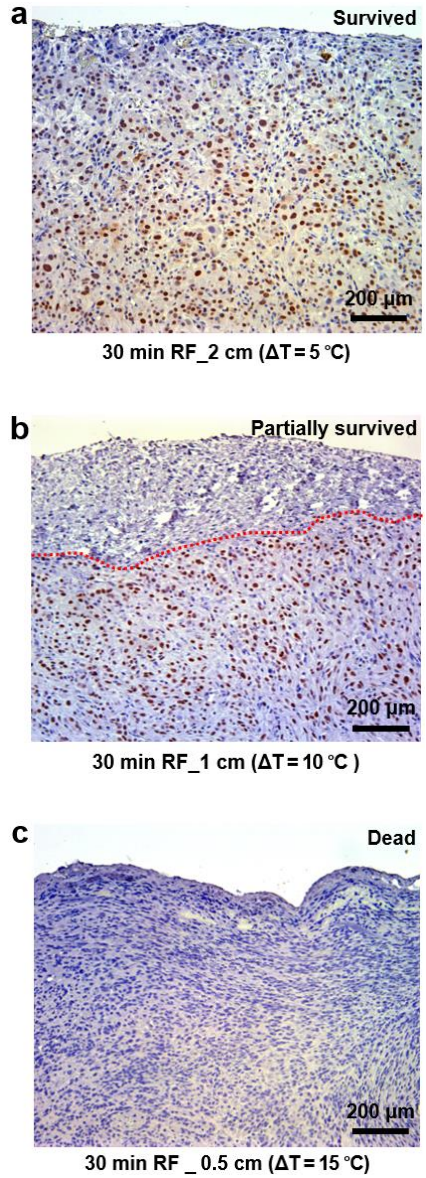

Figure 13. Histological images (survivin) of BEP implanted tumor tissues with 30 min RF heating. Distance between RF coil and BEP is (a) 2 cm, (b) 1 cm, and (c) 0.5 cm.

3.2. Thermal actuation of DOX delivery by bioresorbable heater

Thermal actuation of DOX delivery into biological tissues by Mg heater was investigated both *ex vivo* and *in vivo*. Since DOX has a fluorescence property, diffusion of DOX into bio-tissues can be observed by fluorescence imaging. Figure 14 presents thermally actuated diffusion of DOX into fresh cow brain (*ex vivo*). More accelerated diffusion under higher elevating temperature is appeared.

In vivo study also reveals identical results. Mouse subcutaneous human brain tumor model is used for *in vivo* animal study. Detailed information of the animal model study is described in Experimental Section (5.9). Accelerated delivery of DOX is confirmed by comparing the fluorescence images of DOX diffusion into tumor tissues without and with heating (Figure 15). Without thermal actuation, diffusion length of DOX increases as the implantation time of BEP lengthens, but the amount of released DOX is still insufficient (Figure 15a). On the other hand, fluorescence signal of DOX becomes much stronger if Mg heater is turned on (Figure 15b).

The quantification of DOX concentration depending on the diffusion length was calculated by the integration of equidistant fluorescence intensity from the BEP implant site. Figure 16 shows the implantation time dependent diffusion profile of DOX without thermal actuation. There seem to be only a small increase of diffusion

while the implantation time of BEP lengthens from 0.5 h to 15 h when the heater is turned off. However if the Mg heater is operated, DOX diffusion increased a lot. The effect of enhanced diffusion by thermal actuation is presented in Figure 17. During same period of BEP implantation (15 h), RF heating of 30 min is operated 0, 1, and 4 times for each group. Both the total amount of DOX diffused and the diffusion length are highly increased as the number of thermal actuation performed raises.

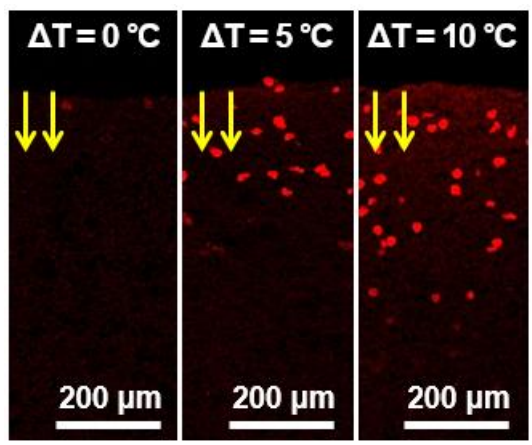

Figure 14. *Ex vivo* fluorescence images of thermally actuated diffusion of DOX into cow brain.

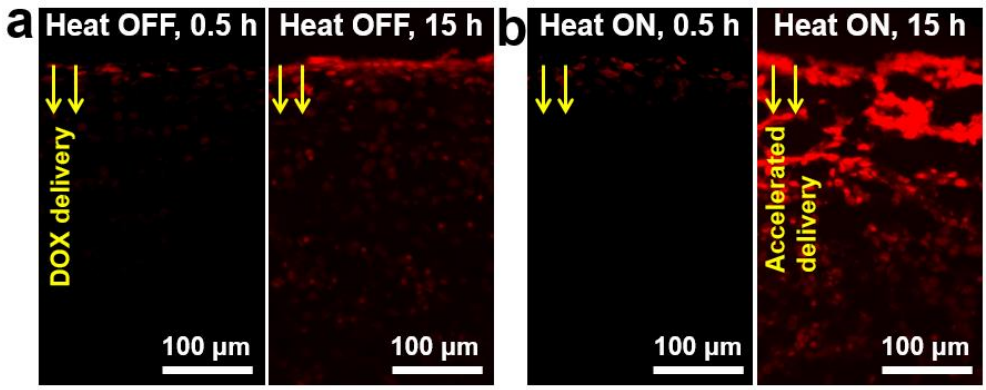

Figure 15. *In vivo* fluorescence images of DOX diffusion into tumor tissues (a) without heating and (b) with heating.

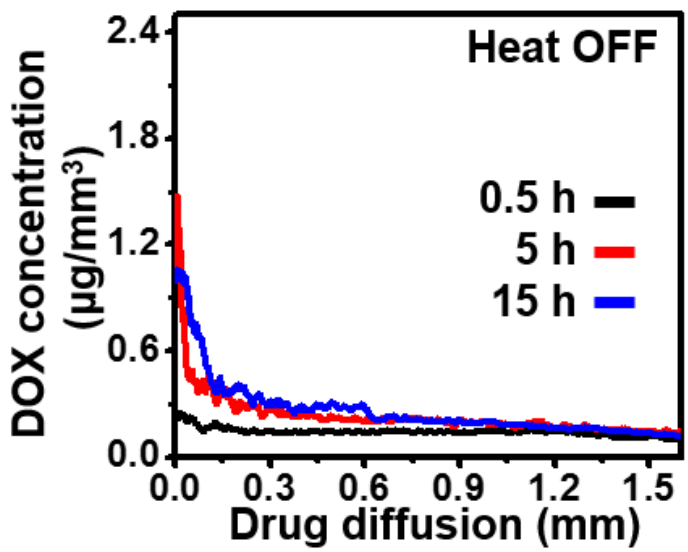

Figure 16. *In vivo* time dependent DOX diffusion profile into tumor tissues without thermal actuation.

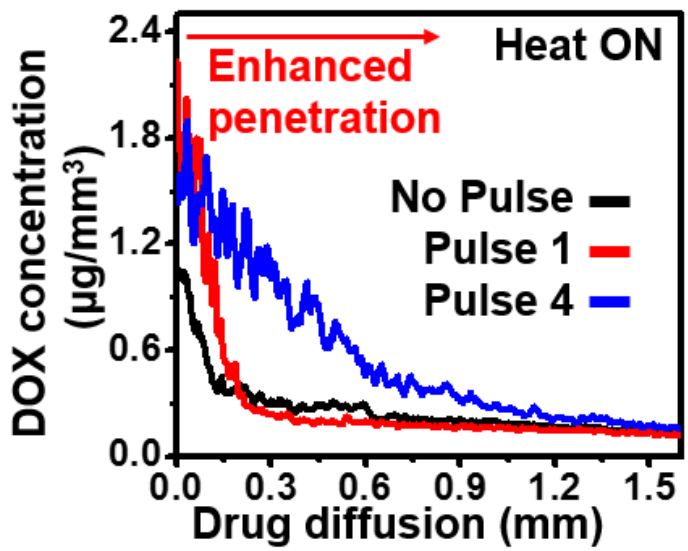

Figure 17. *In vivo* DOX diffusion profile into tumor tissues under thermal actuation by bioresorbable Mg heater. Pulse indicates RF heating of 30 min operated.

3.3. Design and operation of bioresorbable temperature sensor

Since excessive heating may harm normal tissues and cause side effects, real-time temperature monitoring is essential for maintaining proper temperature. Schematic circuit diagram of bioresorbable temperature sensor is described in Scheme 5 and a picture of the sensor is presented in Figure 18 (inset). The sensor is designed as a LC oscillator comprised of Mg line. Bioresorbable polymer, poly lactic-co-glycolic acid (PLGA) that has 65:35 of lactide to glycolide ratio, is used as dielectric materials because its glass transition temperature is about 37 ℃ which is near body temperature. As temperature increases above body temperature, morphology of PLGA changes due to the glass transition resulting in the change of permeability of dielectric. Then resonance frequency of LC oscillator also changes. Temperature change can be detected by observing the movement of resonance frequency of the sensor. Figure 18 shows temperature sensitivity of the sensor. A large movement of resonance frequency is especially observed near body temperature since the morphology of PLGA matrix rapidly alters at that region.

Now, the way to wirelessly detect resonance frequency of the sensor is required. Conventional inductor coil was used as a reader coil. Inductance coupling between the sensor and the reader coil occurs when they are close to each other. As resonance frequency of the sensor affected by the increase of temperature alters, the resonance peak of inductance coupled reader coil also moves (Figure 19). Therefore,

temperature change of BEP can be wirelessly monitored by observing the resonance peak of the reader coil located in parallel with the sensor. Figure 20 shows the result of wireless temperature sensing by using the sensor laminated on the surface of BEP and the reader coil. S11 value of the reader coil at resonance frequency changes as temperature of BEP increases.

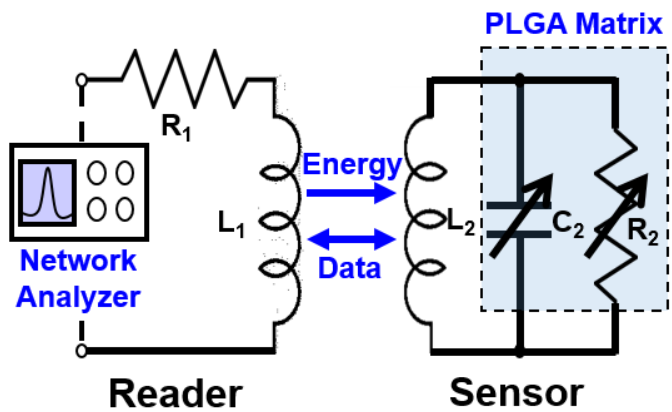

Scheme 5. Schematic circuit diagram of bioresorbable temperature sensor.

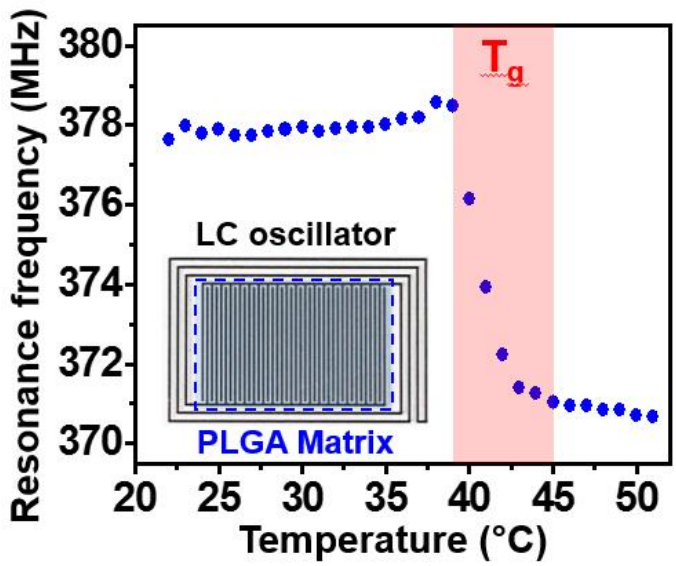

Figure 18. Resonance frequency of bioresorbable temperature sensor as a form of LC oscillator depending on temperature.

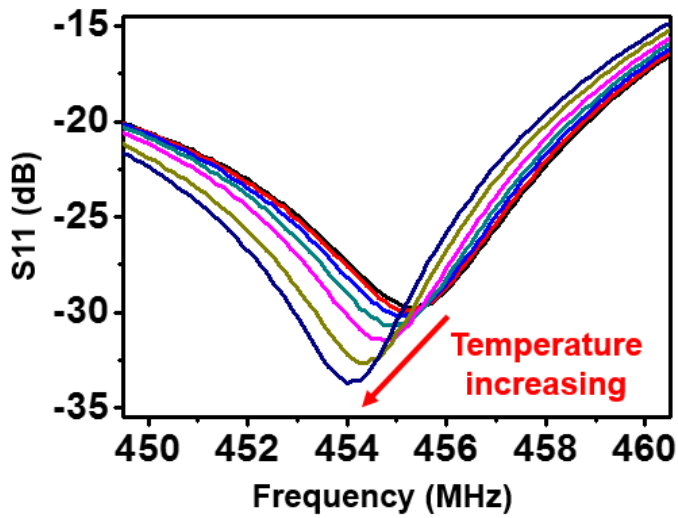

Figure 19. Movement of resonance peak of reader coil as temperature increases.

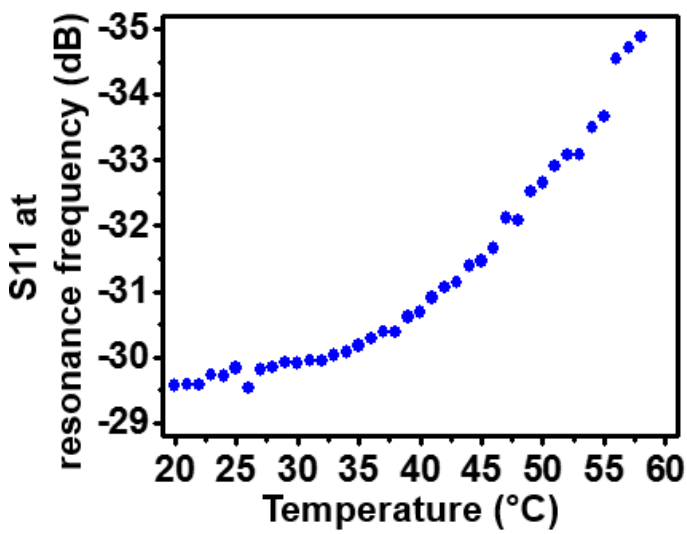

Figure 20. S11 value of reader coil at resonance frequency depending on temperature.

4. *In vivo* demonstration of bioresorbable electronic patch (BEP)

4.1. *In vivo* biocompatibility and bioresorbability of BEP

To investigate biocompatibility and bioresorbability of BEP, histological analyses and MRI study were performed, respectively. Firstly, BEPs were implanted under the subcutaneous tissue of mice. After 7 and 14 days, the tissues containing patch were extracted and stained with H&E and F4/80 antibody which is a macrophage marker. Detailed explanation of immunohistochemistry is in Experimental Section (5.10). Compared to control group in which BEP is not implanted, both the group of BEP implantation for 7 days and 14 days has no discriminable difference of macrophage detection (Figure 21, right). In other words, there is no foreign body reaction or immune reaction of BEP implanted sites.

Bioresorbability of BEP is observed by MRI study. A BEP containing MRI agent was implanted in the rat brain. Then, MRI scanning was done once a week for 4 weeks. Among those images, two MRI images of 1 week (Figure 22a) and 2 weeks (Figure 22b) after implantation, respectively, are introduced as examples. Progression of natural biodegradation of BEP can be observed by comparing two images. More clearly, obtaining 3D images of BEP by an integration of MRI images

facilitate the quantification of bioresorbability (Figure 23a~d). The volume of BEP started with 6.7 mm^3 decreased as time goes by, and finally, became 0.8 mm^3 (Figure 23f). This indicates that approximately four weeks are needed for complete biodegradation of BEP.

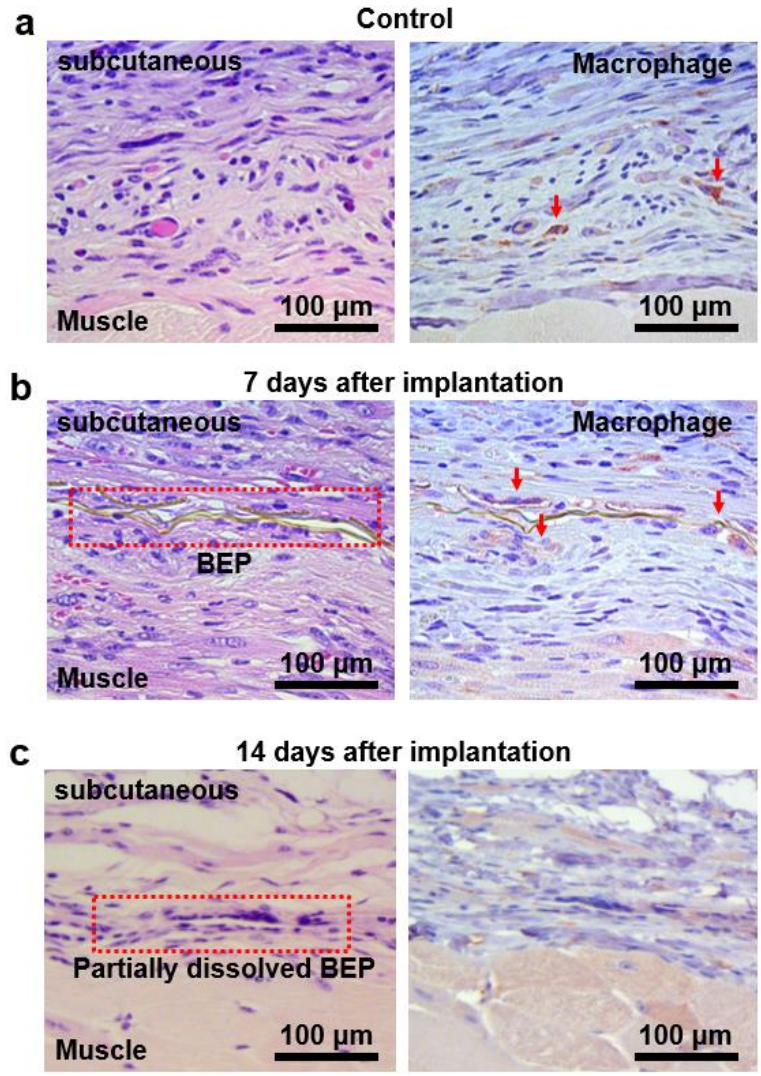

Figure 21. H&E (left) and F4/80 antibody (right) staining images for verifying the biocompatibility of BEP. (a) Control, (b) 7 days after implantation, and (c) 14 days after implantation.

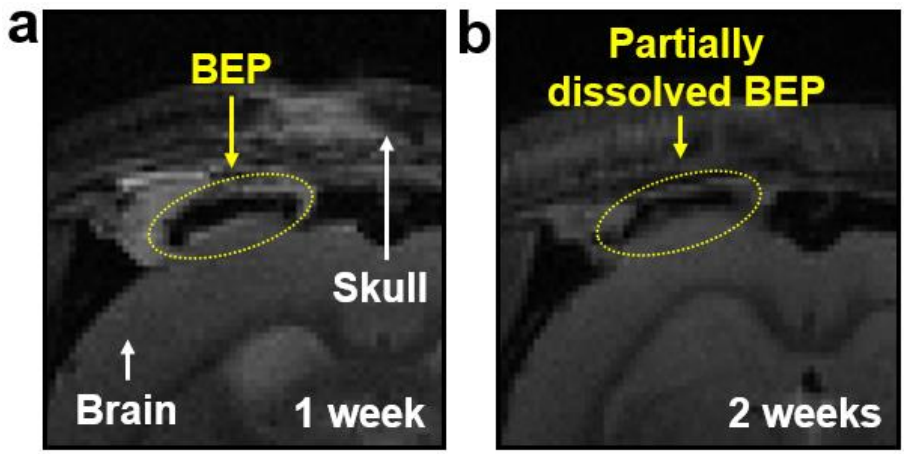

Figure 22. MRI images of BEP implanted rat brain. (a) 1 week and (b) 2 weeks after implantation.

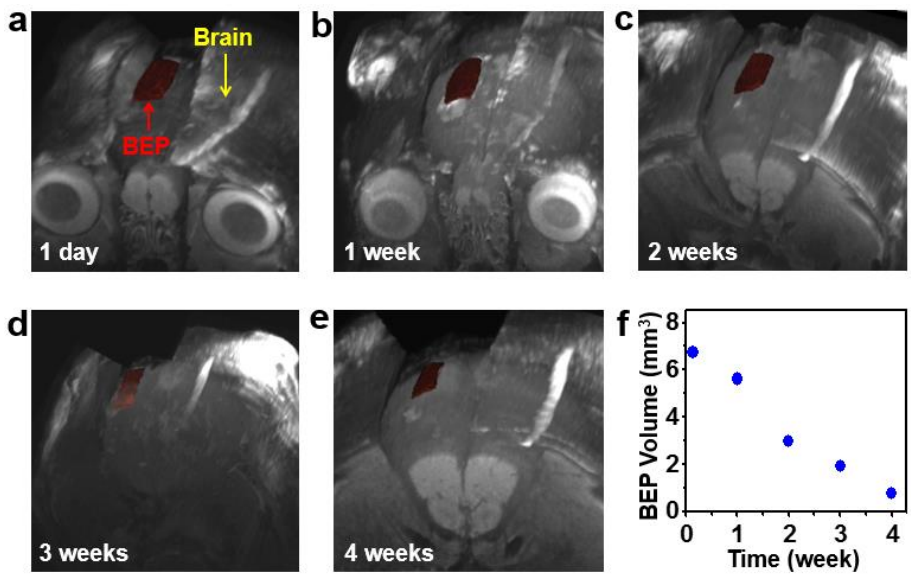

Figure 23. 3D integration of MRI images of rat brain (a) 1 day, (b) 1 week, (c) 2 weeks, (d) 3 weeks, and (e) 4 weeks after BEP implantation and (e) calculated BEP volume.

4.2. BEP treatment procedure of mouse subcutaneous human brain tumor model

To verify therapeutic effects of BEP, treatment using BEP of mouse subcutaneous human brain tumor model was performed. Detailed procedure of treatment is described in Scheme 6. In case of all mice, human brain tumors implanted in subcutaneous tissues were grown to a sphere of ~4 mm radius for 3 weeks and resected to ~20 mm^2 mean residual. Then, a BEP of ~12 mm diameter containing 0.408 mg (0.02 mg/g for body weight of mouse) of doxorubicin was implanted on the residual tumors. For 5 days right after BEP implantation, no RF heating was performed since natural release of drug is enough during the period. After the period, RF heating of 30 min was treated once a day for 2 weeks. During the treatment, the volume of tumors was tracked using MRI every week.

Four different types of treatment groups were set. The group of mice treated by an intravascular injection of an equivalent dosage of DOX (IV), an implantation of BEP with RF heating but containing no DOX (Heater), an implantation of BEP containing DOX but no RF heating (Patch), and an implantation of BEP containing DOX combined with RF heating which is a complete treatment form of BEP (Patch+Heater) were compared. The number of mouse of each group was 6, 7, 7, and 6, respectively. The Heater and Patch+Heater group followed the RF induced heating schedule of treatment procedure (Scheme 6).

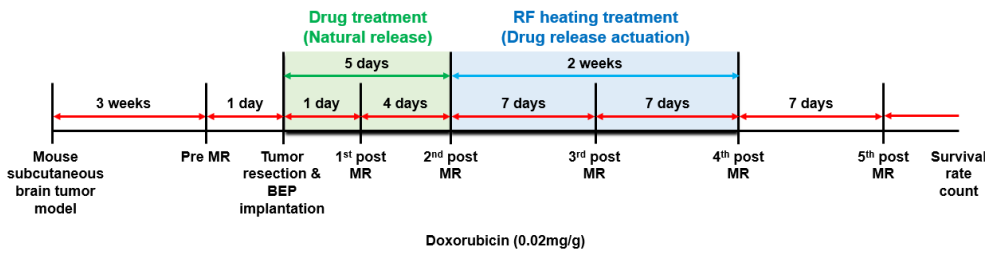

Scheme 6. BEP Treatment procedure of *in vivo* animal study for observing therapeutic effects.

4.3. Tumor recurrence analysis using MRI study

The volume of recurrent tumors observed in MRI images was measured by an ImageJ image analysis. Figure 24 displays the tendency of tumor recurrence of each group by showing representative MRI images of 1 day and 26 days after surgical resection. Quantification of tumor recurrence is shown in Figure 25. Only Patch+Heater group shows the decrease of tumor volume, whereas others reveal significant tumor recurrence. The comparison of final tumor volume of all concerned mice in each group were evaluated by Mann-Whiney U test (Table 1). The Patch+Heater group shows significance compared with all others include Patch (*), Heater (**), and IV (**) groups. The Patch group also shows significance compared with the IV (*) and the Heater (*) group. The Heater and IV groups show no significance (NS) between each other.

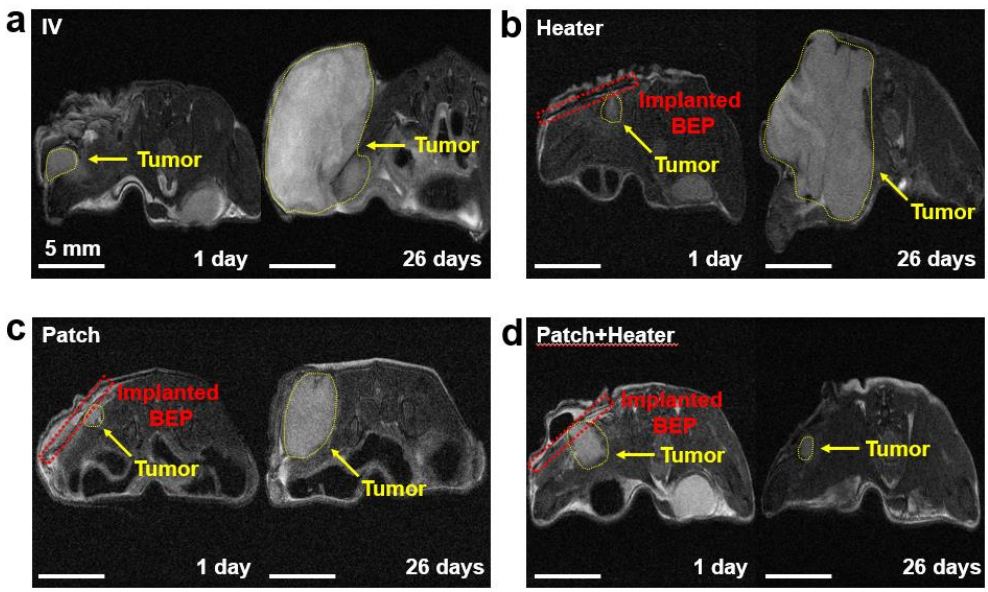

Figure 24. MRI images of recurrent tumors of mouse subcutaneous brain tumor model according to treatment groups. (a) IV represents the group of mice treated by intravascular injection of DOX. (b) Heater represents the group of mice treated by an implantation of BEP with RF heating but containing no DOX. (c) Patch represents the group of mice treated by an implantation of BEP containing DOX but no RF heating. (d) Patch+Heater represents the group of mice treated by an implantation of BEP containing DOX combined with RF heating.

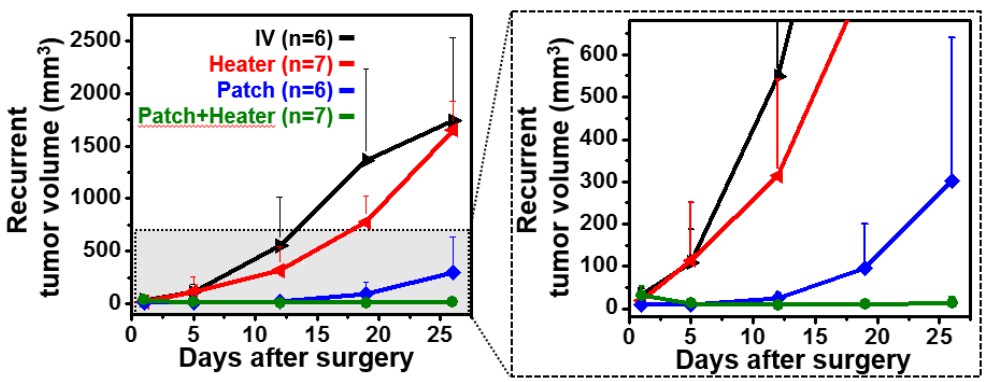

Figure 25. Recurrent tumor volumes versus the time after resection surgery according to treatment groups. Groups are as same as Fig. 24.

	IV	Heater	Patch	Patch+Heater
IV	-	-	-	-
Heater	**NS** ($p = 0.2744^{\S}$)	-	-	-
Patch	* ($p = 0.042^{¶}$)	* ($p = 0.0129^{¶}$)	-	-
Patch+Heater	** ($p = 0.0036^{¶}$)	** ($p = 0.0018^{¶}$)	* ($p = 0.0141^{¶}$)	-

Table 1. Significance of final recurrent tumor volume.

The comparison of final volume of all concerned mice in each group were evaluated by Mann-Whitney U test. * $p < 0.05$, ** $p < 0.01$, NS for no significance.

¶ To compensate for multiple testing, the p value for individual tests was multiplied by the number of comparisons made (Bonferroni correction).

§ When original p-value is large, the corrected p-value is calculated by $1-(1-p)^3$.

4.4. Survival study

Survival study of 60 days after surgical resection was performed for all mice in each group. Figure 26 shows the survival curves of each group. Six mice among seven mice survived longer than 60 days in case of Patch+Heater group, and two mice among six mice of Patch group survived. Meanwhile, all mice are dead before 60 days in case of Heater and IV groups. Statistical analyses are presented in Table 2. The log-rank test was used to compare survival curves. Patch+Heater group shows significance compared with IV (***) and Heater (***) groups and marginal significance (MS) compared with Patch group. Patch group also shows the significance compared with IV (**) and Heater (*) groups. Otherwise, there is no significance (NS) between IV and Heater groups.

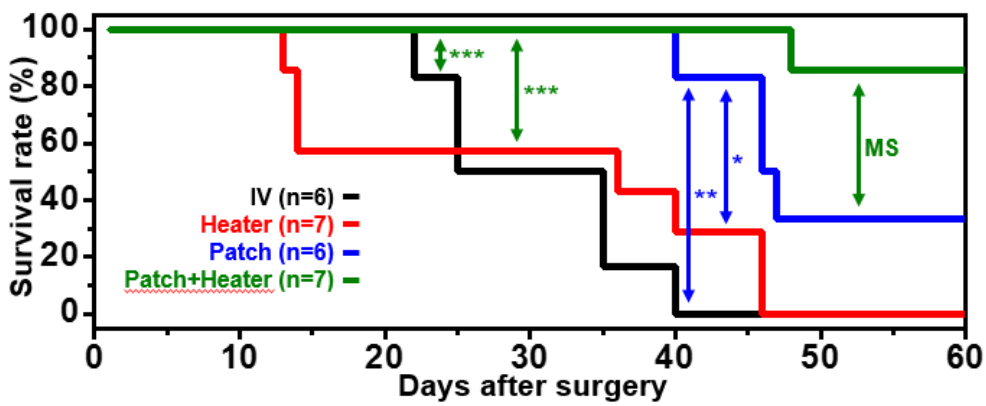

Figure 26. Survival curves according to treatment groups. Groups are as same as Fig. 24.

	IV	Heater	Patch	Patch+Heater
IV	-	-	-	-
Heater	**NS** ($p = 0.9711$§)	-	-	-
Patch	** ($p = 0.0052$¶)	* ($p = 0.0228$¶)	-	-
Patch+Heater	*** ($p = 0.0006$¶)	*** ($p = 0.0006$¶)	**MS** ($p = 0.1016$§)	-

Table 2. Significance of survival study.

The log-rank test was used to compare survival curves. * $p < 0.05$, ** $p < 0.01$, *** $p < 0.001$, NS for no significance, and MS for significance without correction.

¶ To compensate for multiple testing, the p value for individual tests was multiplied by the number of comparisons made (Bonferroni correction).

§ When original p-value is large, the corrected p-value is calculated by $1-(1-p)^3$.

5. Experimental Section

5.1 Materials

Waxy corn starch of essentially pure amylopectin, sodium periodate ($NaIO_4$), poly lactic acid (PLA), Poly lactic-co-glycolic acid (PLGA, lactide:glycolide = 65:35), Phosphate buffered saline (PBS, 0.01M), poly(pyromellitic dianhydride-co-4,4′-oxydianiline)amic acid solution (PI), and 1-metyl-2-pyrrolidinone (NMP) were purchased from Sigma Aldrich (USA). Also, glycerol (Samchun chemical, Korea) was used as a plasticizer and doxorubicin (BK pharm, Korea) were used as an anti-cancer drug. Thermal evaporating source of Mg (Taewon Scientific Co., Korea), sputter target of ZnO (Thifine, USA), polydimethylsiloxane base and curing agent (PDMS, sylgard 184, Dow Corning, USA), Si wafer (4Science, Korea), and positive photoresist S1805, AZ5214, AZ4620 (AZ electronics Materials, USA) were used for the fabrication of bioresorbable electronic heater and temperature sensor.

5.2 Aldehyde functional group modification of starch

Sodium periodate ($NaIO_4$) was used for the synthesis of aldehyde starch. 1 mol of sodium periodate make 1 mol of glucose molecule change their hydroxyl groups into aldehyde groups. Firstly, sodium periodate was dissolved in water. Then,

proper amounts of starch depending on the portion of aldehyde groups on demand was put into the solution. Next, hydrochloric acid was added for making pH of solution into 3 ~ 4. After strong stirring under 40 ℃ overnight, synthesized aldehyde starch was washed with DI water for three times under vacuum. Final products were dried in 40 ℃ oven for 24 hours under vacuum.

5.3 Fabrication of starch patch

In case of normal starch patch containing DOX, proper amounts of starch powder, doxorubicin, glycerol as a plasticizer, and DI water were mixed under high temperature (~80 ℃). Then, mixed solution was dried under appropriate conditions of temperature and humidity (65 ℃ and 80 percentage of humidity) for 24 hours on petri dish.

In case of modified starch patch containing DOX, on the other hand, formation of chemical bonding between starch and DOX is needed first. So, synthesized aldehyde starch and DOX were dissolved in DI water. The mixed solution was strongly stirred under 80 ℃ for 24 hours. Then, glycerol was added to the solution and after an hour, the solution was dried with the same condition as mentioned above.

5.4 Flexibility test of starch patch depending on glycerol contents

Patch samples with different glycerol contents were cut into ~5 mm width and performed the tensile test by a digital force gauge (Mark-10, USA). Both ends of the patch were fixed and stretched at 20 mm/min speed until reaching fracture point. Elastic modulus was calculated from the slope of stress-strain curve. Maximum elongation indicates the elongation at the rupture point.

5.5 Adhesion test of modified starch patch depending on aldehyde contents

Patch samples with different aldehyde contents were cut into ~10 mm width. Then, the patches were attached to the cow muscle instead of brain because brain tissues were so soft that the tissues were torn before the patch was detached when applying the shear stress. The adhesion force was measured by the digital force gauge (Mark-10, USA).

5.6 Measurement of *in vitro* DOX release profile of BEP

All *in vitro* DOX release profiles were obtained by measuring the absorbance of the solution at 480 nm. All patches contained 3.387 mg of DOX with same size (20×20 mm square). Each patch was dipped into 50 mL of 0.01 M phosphate-buffered saline (PBS) solution and 4 samples of 0.1 mL solution each were extracted every measurement time. New 50 mL of PBS solution was replaced everyday right after the sample extraction. Through a prepared standard curve of DOX concentration versus absorbance, released DOX concentration was calculated.

5.7 Fabrication of bioresorbable electronic heater / temperature sensor and transfer of the device to the starch patch

Bottom dilute poly imide (d-PI) film was spin-coated on a Si wafer substrate (3000 rpm, 60 s) and full-cured (200 ℃, over 2 h). Then, a sacrificial layer (poly(methylmethacrylate) (PMMA A11, MicroChem, USA) was spin-coated (3000 rpm, 30s) and cured (180 ℃, 3 min) as a sacrificial layer. About 2 nm of ZnO was deposited as an adhesion layer by AC sputtering at power of 30 W in 15 mTorr Ar atmosphere. 1.5 μm of Mg was then immediately deposited by a thermal evaporator. The deposited Mg was patterned using AZ5214 photoresist (PR) and Mg etchant (mixed solution of nitric acid, water, ethylene glycol; 1:1:3) as the heater and temperature sensor. Top d-PI film was coated again with the same condition as an encapsulation layer. Then, d-PI film was patterned using AZ4620 photoresist (PR) and a reactive-ion etcher (RIE). PMMA film was undercut by acetone and the device was picked-up by 10:1 PDMS stamp (sylgard 184, Dow Corning, USA). Bottom d-PI layer was etched by RIE on PDMS stamp.

To transfer the device on PDMS stamp onto the starch patch, PLA was spin-coated (3000 rpm, 30 s) on the top surface of the starch patch. A drop of chloroform was fallen onto the surface of the starch patch. Then, the device was transferred from the PDMS stamp to the starch patch. After the transfer, top d-PI layer was etched by

RIE. Finally, PLA was spin-coated (500 rpm, 30 s) again as a top encapsulation layer for protecting Mg device.

5.8 Doxorubicin assessment

After the experiment ends, implanted BEP was retrieved and tumor was extracted. Tissue blocks of the entire tumor were cut, embedded in OCT compound, and stored at −80 ℃. Ten thin (10 μm) serial frozen sections were obtained for doxorubicin assessment and the cryosections were imagined by fluorescence microscopy (magnification, ×100; LSM 510 META, Carl Zeiss, Oberkochen, Germany) with filter sets for doxorubicin (excitation/emission: 488/520 nm; exposure time: 4 s).

5.9 Animal model study

All animal experiments were approved by the Institutional Animal Care and Use Committees of Seoul National University Hospital (Approval number. 14-0156-C1A3). Human glioblastoma cell line U-87 MG was obtained from the American Type Culture Collection (ATCC, Rockville, MD, USA) and maintained in RPMI medium with 10 % FBS at 37 ℃. All cell lines were re-authenticated by microsatellite profiling immediately before manuscript submission. U-87 MG glioblastoma cells were prepared in 100 mL serum- free RPMI and then subcutaneously transplanted into the shoulders of 6-week old BALB/c nude mice (n=26; $2x10^6$ cells/100 mL medium/each mouse). After 2 weeks after injection, mice

were imaged with MRI to determine tumor size and location for pre-surgical planning.

5.10 Immunohistochemical staining

Immunohistochemical staining was performed using formalin-fixed paraffin-embedded tumor blocks. Briefly, 4-µm-thick tissue sections were deparaffinized in xylene and hydrated by immersing in a series of graded ethanol. Antigen retrieval was performed in a microwave by placing the sections in epitope retrieval solution (0.01 M citrate buffer, pH 6.0) for 20 minutes; endogenous peroxidase was inhibited by immersing the sections in 0.3 % hydrogen peroxide for 10 minutes. Sections were then incubated with primary rabbit polyclonal antibody to F4/80 (Santa cruz) for inflammatory macrophages or rabbit monoclonal antibody to Survivin (Cell signaling) in Dako REAL antibody diluent (Dako). Staining for the detection of bound antibody was evaluated by DAB.

5.11 Magnetic resonance imaging (MRI) protocol

For the *in vivo* animal MR study, the tail vein was catheterized after anesthesia with 1.5-2 % isoflurane/oxygen (v/v), and the animals were placed in the 9.4T MR scanner (Agilent Technologies). Throughout each imaging session, animals were wrapped in a warm water blanket and oxygen saturation and heart rate were monitored. A Milliped Coil (1-ch coil (Both RF transmission and signal

reception); Agilent Technologies, Santa Clara, CA, USA) and a FSE (Fast Spin Echo) sequence for T2-weighted image was used. The measurement parameters were as follows: TR = 3000 ms, effective TE = 30.82 ms, FOV = 20×35 mm, ETL = 4, matrix = 256×256, slice thickness = 1.0 mm.

6. Conclusion

In summary, a natural bioresorbable polymer, starch, was fabricated as a form of flexible patch having good adhesion to biological tissues and loading an anti-cancer drug named doxorubicin (DOX). Aldehyde functional group modification of starch facilitated delayed, localized, and tumor targeted drug delivery of patch. Electronic components include heater and temperature sensor were fabricated by using bioresorbable metal (Mg) and polymer (PLGA) and laminated on the surface of starch patch. Wireless RF heating of the heater was confirmed that DOX diffusion can be thermally accelerated. The temperature sensor as a form of LC oscillator wirelessly detected the temperature of BEP so that excessive heating can be prevented. Biocompatibility and bioresorbability of BEP was investigated *in vivo*. Therapeutic effects were also verified by tumor recurrence analysis using MRI and survival study. Statistical analyses showed that the therapeutic effect of BEP treatment is significant compared with other control groups. Therefore, this bioresorbable electronic patch (BEP) enabled active control of drug delivery can be suggested as a novel form of treatment of brain tumor disease.

7. References

1. Krex, D., Klink, B., Hartmann, C., von Deimling, A., Pietsch, T., Simon, M., ... & Weller, M. (2007). Long-term survival with glioblastoma multiforme. *Brain*, ***130*(10)**, 2596-2606.

2. Mrugala, M. M. Advances and challenges in the treatment of glioblastoma: a clinician's perspective. *Discov Med*. ***15*(83)**, 221-230, (2013)

3. Stummer, W., Pichlmeier, U., Meinel, T., Wiestler, O. D., Zanella, F., Reulen, H. J., & ALA-Glioma Study Group. (2006). Fluorescence-guided surgery with 5-aminolevulinic acid for resection of malignant glioma: a randomised controlled multicentre phase III trial. *The lancet oncology*, ***7*(5)**, 392-401.

4. Lesniak, M. S., & Brem, H. (2004). Targeted therapy for brain tumours. *Nature reviews Drug discovery*, ***3*(6)**, 499-508.

5. Silva, A. C., Oliveira, T. R., Mamani, J. B., Malheiros, S. M., Malavolta, L., Pavon, L. F., ... & Martins, M. J. (2011). Application of hyperthermia induced by superparamagnetic iron oxide nanoparticles in glioma treatment. *Int J Nanomedicine*, ***6*(3)**, 591-603.

6. Hayashi, K., Nakamura, M., Sakamoto, W., Yogo, T., Miki, H., Ozaki, S., ... & Ishimura, K. (2013). Superparamagnetic nanoparticle clusters for cancer

theranostics combining magnetic resonance imaging and hyperthermia treatment. *Theranostics*, ***3*****(6)**, 366-376.

7. Kumar, C. S., & Mohammad, F. (2011). Magnetic nanomaterials for hyperthermia-based therapy and controlled drug delivery. *Advanced drug delivery reviews*, ***63*****(9)**, 789-808.

8. Abel, T. J., Ryken, T., Lesniak, M. S., & Gabikian, P. (2013). Gliadel for brain metastasis. *Surgical neurology international*, ***4*****(Suppl 4)**, S289.

9. Ratnayake, W. S., & Jackson, D. S. (2006). Gelatinization and solubility of corn starch during heating in excess water: new insights. *Journal of Agricultural and Food Chemistry*, ***54*****(10)**, 3712-3716.

10. Yu, J., Chang, P. R., & Ma, X. (2010). The preparation and properties of dialdehyde starch and thermoplastic dialdehyde starch. *Carbohydrate polymers*, ***79*****(2)**, 296-300.

11. Bagheri, S., Hassani, S. M., & Ghahremani, H. (2012). Computational Procedure for Determining Physicochemical Properties of Doxorubicin-TPGS and Daunorubicin-TPGS as Anticancer Agents. *Oriental Journal of Chemistry*, ***28*****(2)**, 835.

12. Yu, D., Xiao, S., Tong, C., Chen, L., & Liu, X. (2007). Dialdehyde starch nanoparticles: Preparation and application in drug carrier. *Chinese Science Bulletin*, ***52*****(21)**, 2913-2918.

13. Kirdant, A. S., Shelke, V. A., Shankarwar, S. G., Shankarwar, A. G., & Chondhekar, T. K. (2011). Kinetic study of hydrolysis of N-salicylidene-m-methyl aniline spectrophotomerically. *J. Chem. Pharm. Res*, ***3***, 790-796.

14. Hassib, H. B., Abdel-Kader, N. S., & Issa, Y. M. (2012). Kinetic Study of the Hydrolysis of Schiff Bases Derived from 2-Aminothiophenol. *Journal of solution chemistry*, ***41*****(11)**, 2036-2046.

15. Yu, Y., Chen, C. K., Law, W. C., Weinheimer, E., Sengupta, S., Prasad, P. N., & Cheng, C. (2014). Polylactide-graft-doxorubicin nanoparticles with precisely controlled drug loading for pH-triggered drug delivery. *Biomacromolecules*, ***15*****(2)**, 524-532.

16. Xiao, N., Liang, H., & Lu, J. (2011). Degradable and biocompatible aldehyde-functionalized glycopolymer conjugated with doxorubicin via acid-labile Schiff base linkage for pH-triggered drug release. *Soft Matter*, ***7*****(22)**, 10834-10840.

요약 (국문초록)

뇌종양 치료를 위한 능동적인 약물 전달 조절이 가능한 생분해성 전자 패치

서울대학교 공과대학원

화학생물공학부

서현선

뇌종양은 가장 치료하기 어려운 암 중 하나이다. 뇌로의 약물전달을 가로막는 혈뇌 장벽의 존재와 종양제거 수술 후의 잔여 암 조직으로 인해 뇌종양은 아직까지도 해결 불가능한 질병으로 남아 있다. 최근 기존의 뇌종양 치료방법의 한계를 극복하기 위한 노력들이 보고되고 있다. 대표적으로 생분해성 고분자 웨이퍼를 이용한 체내 삽입형 약물전달 시스템이 임상적으로 사용되고 있으나 약물 전달이 조절 불가능하며 비효율적이라는 치명적인 단점이 있다. 이 때문에 능동적으로 조절 가능한 새로운 약물 전달 시스템의 필요성이 대두되고

있다. 본 논문에서는 뇌종양치료를 위한 지속적이고 조절가능하며 국지적인 약물전달이 가능한 생분해성 전자 패치를 개발하였다. 생분해성 천연 고분자인 녹말을 유연한 패치의 형태로 가공하여 생체조직과 밀접한 접촉이 가능하게 하고, 여기에 항암제인 독소루비신을 담지하였다. 녹말 고분자의 작용기 치환을 통해 독소루비신과 녹말 사이에 공유결합을 형성시켜 약물의 자연 방출 속도를 감소시켰다. 생분해성 금속인 마그네슘으로 만들어진 히터를 통한 무선주파수 유도 가열은 이러한 공유결합을 끊어 약물 전달을 열적으로 촉진시킬 수 있다. 과도한 가열을 방지하기 위해 엘씨 발진기 형태의 무선온도센서를 통해 실시간 온도 감지를 수행하였다. MRI를 통한 종양의 재발 분석과 생존율 분석을 통해 생분해성 전자 패치의 치료효과를 검증하였다. 이를 통해 새롭고 효과적인 뇌종양 치료방법으로서 능동적 약물 전달이 가능한 생분해성 전자 패치의 잠재력을 확인할 수 있었다.

주요어: 생분해성 패치, 생분해성 전자소자, 뇌종양 치료, 삽입형 약물 전달 시스템.

학번: 2014-22593